Projecting global mangrove species and community distributions under climate change

S. Record,[1,4],† N. D. Charney,[2] R. M. Zakaria,[3] and A. M. Ellison[1]

[1]*Harvard Forest, Harvard University, Petersham, Massachusetts 01366 USA*
[2]*School of Natural Sciences, Hampshire College, Amherst, Massachusetts 01002 USA*
[3]*Institute of Biological Sciences and Institute of Ocean and Earth Sciences, University of Malaya,
Kuala Lumpur 50603 Malaysia*

Abstract.   Given the multitude of ecosystem services provided by mangroves, it is important to understand their potential responses to global climate change. Extensive reviews of the literature and manipulative experiments suggest that mangroves will be impacted by climate change, but few studies have tested these predictions over large scales using statistical models. We provide the first example of applying species and community distribution models (SDMs and CDMs, respectively) to coastal mangroves worldwide. Species distributions were modeled as ensemble forecasts using BIOMOD. Distributions of mangrove communities with high species richness were modeled in three ways: as the sum of the separate SDM outputs, as binary hotspots (with >3 species) using a generalized linear model, and continuously using a general boosted model. Individual SDMs were projected for 12 species with sufficient data and CDMs were projected for 30 species into 2080 using global climate model outputs and a range of sea-level rise projections. Species projected to shift their ranges polewards by at least 2 degrees of latitude consistently experience a decrease in the amount of suitable coastal area available to them. Central America and the Caribbean are forecast to lose more mangrove species than other parts of the world. We found that the extent and grain size, at which continuous CDM outputs are examined, independent of the grain size at which the models operate, can dramatically influence the number of pseudo-absences needed for optimal parameterization. The SDMs and CDMs presented here provide a first approximation of how mangroves will respond to climate change given simple correlative relationships between occurrence records and environmental data. Additional, precise georeferenced data on mangrove localities and concerted efforts to collect data on ecological processes across large-scale climatic gradients will enable future research to improve upon these correlative models.

Key words: climate envelope; community; global; mangal; sea-level rise; species richness.

[4] Present address: Department of Biological Sciences, Smith College, Northampton, Massachusetts 01063 USA.
† **E-mail:** srecord@smith.edu

INTRODUCTION

Sea-level rise and altered weather patterns resulting from global climate change have impacted and will continue to impact coastal systems, altering the ecological and economic services that they offer (Nicholls et al. 2007). In coastal tropical and sub-tropical areas throughout the world, salt-tolerant mangrove trees are of vital ecological and societal importance (re-

viewed by Walters et al. 2008). For instance, mangroves have the ability to sequester five times the amount of carbon than upland tropical forests (Siikamäki et al. 2012). Mangroves also provide critical habitat for organisms occupying the land-sea interface (Ellison 2008). Seafood production in many developing and developed countries throughout the world relies directly or indirectly on mangroves (Rönnbäck 1999, Ellison 2008). Mangroves may also provide a buffer that protects coastal and nearby inland human settlements from erosion and tropical storm damage (Das and Vincent 2009).

To better understand the uncertainty in projecting the global economic potential for decreasing carbon dioxide emissions from mangrove loss and because many other ecosystem services provided by mangroves also are affected by the diversity and distribution of mangroves, it is important to understand how large-scale patterns in their distributions are likely to respond to global climatic change (Ellison 1993, Ellison 2002). Extensive reviews of the literature summarize relationships between mangroves and environmental drivers in contemporary and historic times to speculate on how global climate change might affect mangroves worldwide (Ellison 1994, Snedaker 1995, Alongi 2008, Gilman et al. 2008). Manipulative laboratory experiments have explored fine-scale responses of mangroves to drivers associated with global climate change (e.g., elevated sea level and CO_2 concentrations) (Farnsworth et al. 1996, Ellison and Farnsworth 1997, Ye et al. 2003). These reviews and experiments suggest that individual mangrove species' distributions may contract and local species richness and productivity may decrease in regions where climate-change scenarios forecast that precipitation and run-off will decrease while salinity soil sulfides increase (Ellison 1994, Snedaker 1995). In contrast, where precipitation and run-off increase, upland nutrients will be deposited, salinity will be reduced, and acid-sulfide soils will be moderated, leading to increased productivity, opportunities for range expansion of individual mangrove species, and potential for increases in local species richness. Latitudinal range limits of mangroves are forecast to increase as air temperatures warm; current mangrove distributions are limited by the 16°C isotherm of the coldest month (Ellison

1994, Gilman et al. 2008).

Manipulative experiments and literature-based predictions of range and compositional shifts suggest hypotheses of how mangroves will respond to climate change that can be addressed using large-scale (macroecological) statistical models that directly relate future climate-change to mangrove distributions (Ellison 2002). Although they have not been widely applied to mangroves (cf. Gilman et al. 2007 for an example of a regional study), species and community distribution models (SDMs and CDMs, respectively) are a common tool used by macroecologists to assess potential threats of climate change to biodiversity (e.g., Fitzpatrick et al. 2011). These models use simple correlative relationships between species occurrences or indices of community composition and current environmental data to extrapolate species (or community) distributions across space and/or time (Guisan and Thuiller 2005, Peterson et al. 2011). While such SDMs and CDMs do not incorporate many ecologically relevant factors (e.g., biotic interactions, evolutionary change), they do provide a first approximation for thinking about the large-scale impacts of climate change on organisms (Pearson and Dawson 2003).

Previous mangrove modeling research has focused on topics such as mangrove demography (Clarke 1995), distributions (Cohen et al. 2005), stand dynamics (Chen and Twilley 1998, Twilley et al. 1999, Berger and Hildenbrandt 2000; individual-based models reviewed by Berger et al. 2008), ecosystem function and services (Heald 1971, Grasso 1998), and food webs (Odum and Heald 1975) at geographic extents much smaller than the range of a species. Here we use SDMs and CDMs to explore how mangrove biodiversity may respond to global climatic change at large spatial extents encompassing the entirety of species' ranges. SDMs generate detailed information on potential ranges of individual species, but are meaningful only when data are extensive (Fitzpatrick et al. 2011). In contrast, CDMs provide additional insights into rare species because they are capable of including infrequently sampled species. Of the SDMs we ask: (1) will each species' coastal range expand, contract, or remain the same; and (2) if the species' range does change, does it shift poleward or towards the equator? We use CDMs to ask: (1) will there

Table 1. List of the 30 mangrove species for which there were data in the Global Biodiversity Information Facility (GBIF) database.

Species	Abbreviation	No. GBIF records	No. modeled grid cells
Avicennia alba Blume	AVAL	15	11
A.bicolor Standley	AVBI	156	43
A. eucalyptifolia (Zipp. ex Miq.) Moldenke	AVEU	20	12
A. germinans (L.) Stearn†	AVGE	1569	569
A. integra Duke	AVIN	5	3
A. lanata Ridley	AVLA	1	1
A. marina (Forssk.) Vierh.†	AVMA	1244	394
A. schaueriana Stapf. & Leechman ex Moldenke	AVSC	4	3
Ceriops australis	CEAU	72	45
C. decandra (Griff.) Ding Hou	CEDE	23	19
C. tagal (Perr) c.B. Robinson†	CETA	196	142
Kandelia candel (L.) Druce	KACA	72	23
K. obovata Sheue, Liu & Yong	KAOB	30	7
Laguncularia racemosa (L.) Gaertn. F.†	LARA	1385	556
Lumnitzera littorea (Jack) Voigt†	LULI	72	56
L. racemosa Willd.†	LURA	184	137
Nypa fruticans (Thunb.) Wurmb.	NYFR	37	24
Rhizophora apiculata Bl.†	RHAP	85	59
R. harrisonii Leechman	RHHA	29	13
R. mangle Guppy†	RHMA	1166	528
R. mucronata Lamk.†	RHMU	126	75
R. racemosa Meyer†	RHRA	227	89
R. stylosa Griff.†	RHST	167	118
R. x. harrisonii Leechman	RHHAx	33	13
R. x. lamarckii Montr.	RHLAx	7	7
Sonneratia alba J. Smith†	SOAL	127	89
S. apetala Buch. -Ham.	SOAP	2	1
S. caseolaris (L.) Engler	SOCA	36	31
S. ovate Backer	SOOV	6	2
S. x. gulngai N.C. Duke	SOGUx	2	1

Note: Abbreviated names follow a 4-5 letter naming convention (first two letters of the generic and specific epithets followed by a lowercase 'x' for hybrids). Modeled grid cells were 2.5 minutes in size. Tables 2 and 3 and Fig. 2 refer to the abbreviated names.

† These species had >50 occupied 2.5 minute resolution grid cells and were modeled by the individual species distribution models.

be poleward shifts in areas with multiple mangrove species; and (2) given reasonable scenarios of climatic change, where do we forecast gains and losses in mangrove species richness?

METHODS

Mangrove occurrence data

We focus our analyses on 30 species in the eight major mangrove genera (sensu Tomlinson 1986) that contribute most to the community structure in mangrove forests and provide the majority of ecosystem services (Rönnbäck 1999, Khatiresan and Bingham 2001, Ellison 2008). Mangrove occurrence (presence-only) data (Table 1) were obtained from the Global Biodiversity and Information Facility Database (GBIF: http://www.gbif.org; Appendix), and included data from museum specimens, peer-reviewed papers,

and the Mangrove Database of the Flanders Marine Institute (http://www.vliz.be/vmcdata/mangroves). Occurrence records were checked against species distribution maps (Spalding et al. 2010); outliers (including living specimens in botanic gardens) were removed before analysis (cf. Yesson et al. 2007).

We limited our modeling to coastal regions because mangroves are primarily coastal (Tomlinson 1986). We generated global coastal GIS layers by applying the "contour list" tool in ArcMAP 9.3 to a global topography and bathymetry digital elevation model (http://www.ngdc.noaa.gov). We generated coastlines at 0, 1, 3, and 6 m contours, which correspond respectively to the current coastline and three projected increases in global sea-level. A 1-m rise corresponds to the upper limits of forecasted sea-level rise not accounting for rapid dynamical changes

in ice-mass loss (IPCC 2007). Given the uncertainty in the magnitude of ice-mass loss in areas such as Greenland over the next 100 years, however, we also modeled 3 and 6 m rises in sea-level (Bromwich and Nicolas 2010).

The coastal GIS layers were converted to 2.5-minute resolution (4,318 m grid cells) in a Goode homolosine projection for all subsequent modeling. A 2.5 minute resolution balances a sufficiently fine scale for non-climatic predictors (e.g., horizontal tide, river discharge) with computational resources. All GBIF data within 40 km of the coastline were assigned to the nearest grid cell of the current coast; these occurrence records yielded 7,085 unique records distributed across 1,847 grid cells that were used in the models, which treated each coastal grid cell as an observation unit. All data used in this study are available online through the Harvard Forest Data Archives (http://harvardforest.fas.harvard.edu/data-archives).

Environmental predictors

We compiled a data set of 21 climatic, hydrological, and geomorphological variables associated with mangrove distribution patterns (Duke et al. 1998, Gilman et al. 2007, Alongi 2008). Bioclimatic variables were obtained from the WorldClim database (http://www.worldclim.org). These nineteen variables include summary statistics for temperature and rainfall (e.g., mean, range) at different temporal resolutions (e.g., annually, quarter annually) and represent average climatic conditions from 1950–2000 interpolated from weather station data. We refer to these data as "current" climate data (Hijmans et al. 2005). Estimates of horizontal tide and river discharge were based on catchment size. Horizontal tide was estimated by dividing the vertical tidal amplitude by slope, where vertical tides were obtained by summing the primary tidal amplitude constituents, M2 and K1 (Lyard et al. 2006), obtained from the NASA Planetary Geodynamics Lab, and slope was obtained from the global bathymetry and topography digital elevation model. River discharge was obtained using the "Flow Accumulation" tool in ArcMAP 9.3 applied to a global topography layer; flow accumulation was weighted by mean annual rainfall for the current and future scenarios.

For each of the 21 predictors, we used WorldClim data to generate a corresponding set of future environmental values based on the 2080 projections of the National Center for Atmospheric Research's (NCAR) CCSM3 general circulation model (GCM) under the Intergovernmental Panel on Climate Change IV's SRES A1b scenario. We chose this rapid growth, carbon intensive scenario because observed data on global fossil fuel emissions increased from 2000–2008 by 29%, suggesting that despite efforts to stabilize CO_2 emissions to curtail global climatic change our planet is experiencing the more extreme of the SRES scenarios (Le Quéré et al. 2009). This GCM forecasts a +2°C change in annual temperature within the current latitudinal limits of mangroves (32° N and 40° S; Spalding et al. 2010). Precipitation projections are more variable; some mangrove areas are forecast to have 50% less annual precipitation (most of Central America and the Caribbean), whereas other areas are forecast to have 50% more (most of Southeast Asia). Although we recognize that there also is variation among GCMs (IPCC 2007), it was beyond the scope of this study to run different GCMs on the SRES A1b scenario.

As we did for the mangrove occurrence data, we assigned to each coastal grid cell the nearest value (within a 40-km radius) of each of the current and future environmental variables. To account for possible spatial error in the river discharge layer to coastal cells, this layer was first resampled at a 14 km grid size, taking the maximum value within that larger region before assigning values to the coastal cells.

Species distribution modeling

We used BIOMOD (Thuiller et al. 2009) to generate SDMs for the 12 mangrove species that occurred in at least 50 modeled grid cells (Table 1). Note that while there were 15 species in the GBIF data with >50 occurrences, there were only 12 species with >50 occupied 2.5 minute resolution grid cells. Outputs of SDMs and CDMs are sensitive to the type of statistical model fit to the occurrence data, so it is preferable to fit many statistical models to the data and combine them into an "ensemble forecast" (Araujo and New 2007). BIOMOD generates ensemble forecasts of species distributions based on contributions from multiple statistical models and initial conditions. We fit

and compared all nine of the statistical models available in BIOMOD R2.14: generalized linear models, generalized boosting models, classification and regression trees, generalized additive models, artificial neural networks, surface range envelopes, flexible discriminant analyses, multiple adaptive regression splines, and random forests (detailed in Thuiller et al. 2009, R Development Core Team 2011).

BIOMOD models require both presence and absence data. Creating pseudo-absences (i.e., background absences) is common when fitting SDMs because presence only data often are obtained from herbaria records or online databases, so pseudo-absences are generated to better characterize the set of environmental conditions a specie's experiences within its current range (Thuiller et al. 2009). The results of SDMs can be sensitive to the selection of pseudo-absences, the ratio of presences to pseudo-absences, and the geographic extent of pseudo-absences (Lobo et al. 2010, Barbet-Massin et al. 2012). We therefore used several approaches to generating pseudo-absences to accompany our presence-only data on mangroves. One approach we used for selecting pseudo-absences was to use all locations within 40 kilometers of the coastline in the entire mangrove occurrence data set as absences, including locations where the focal species had been found. Phillips et al. (2009) showed that including localities with known occurrences as pseudo-absences helps to minimize spatial bias in survey effort (i.e., bias due to some areas being easier to access and sample for presences than other areas). Random selection of pseudo-absences is a common method (Stockwell and Peters 1999, Fitzpatrick et al. 2011), and the selection of a large number of pseudo-absences at random has been shown to have better predictive performance than more sophisticated methods based on fitting a preliminary model to identify areas of low habitat suitability (Wisz and Guisan 2009). We generated a random selection of 500, 1000, and 10,000 locations within 40 kilometers of the coastline between latitudes 47° S and 47° N, with an equal weight of presence to background data. The geographic extent of the pseudo-absence locations was limited to a lower latitude area of the world because previous studies found that artificial absences that were too far from the presence locations in environmental space were

not helpful in differentiating suitable from non-suitable conditions (Lobo et al. 2010, Barbet-Massin et al. 2012).

To avoid model over-fitting and to identify the most important current climate environmental variables associated with mangrove distributions, we used generalized boosted models (GBMs) for each species within BIOMOD. GBMs allow for correlated predictors and average across all regression trees created by the boosting algorithm to give robust estimates of the relative importance of each environmental predictor in the model (Friedman 2001, Elith et al. 2008). To reduce uncertainties due to the method used to generate pseudo-absences and due to the stochastic nature of the GBM algorithm, ten GBMs were fit for each of the four pseudo-absence data sets (a total of 40 GBMs). The average relative importance of each predictor over these 40 GBMs was then used to identify the five most important predictor variables for each species to be used in the final SDMs (following Friedman 2001) (Tables 2 and 3). For weights in these and the final models, we used the total number of occurrence records for each species per grid cell.

These top five most important variables for each species were then used to fit the statistical models in BIOMOD for each combination of presence/pseudo-absence data. Data combinations were split randomly ten times into calibration (70%) and evaluation (30%) components, and the models were run on each of the ten calibrations and evaluation data sets. We assessed the predictive performance of each of the SDMs with the True Skill Statistic (TSS) as it is independent of prevalence (i.e., the proportion of locations with presences) and it accounts for omission and commission errors (i.e., false negatives and false positives, respectively) (Allouche et al. 2006). TSS ranges from -1 to $+1$; a value of $+1$ indicates perfect agreement between model predictions and the validation data, whereas values <0 indicate model predictions no better than random. We present here the ensemble forecast for the current climatic conditions and future scenarios from models fit using presence/500 random pseudo-absence data, because this combination yielded the highest TSS value. The contribution of each statistical model to the ensemble was based on a weighted average in which the relative weight of the

Table 2. The five most important environmental predictors identified by general boosted models and the exclusion of correlated variables for *Avicennia germinans* (AVGE), *A. marina* (AVMA), *Ceriops tagal* (CETA), *Laguncularia racemosa* (LARA), *Lumnitzera littorea* (LULI), and *L. racemosa* (LURA). All of these species' individual distributions were modeled.

Bioclimatic variable	AVGE	AVMA	CETA	LARA	LULI	LURA
Annual mean temp.	1	...	...	...	...	...
Mean diurnal range	2	...	...	3	4	...
Isothermality	...	3	5	2	...	...
Temp. seasonality	...	...	...	...	...	...
Max. temp. of warmest month	...	5	...	1	...	...
Min. temp. of coldest month	...	...	...	...	...	...
Temp. annual range	...	...	...	...	...	...
Mean temp. of wettest quarter	...	4	1	...	...	2
Mean temp. of driest quarter	...	1	3	2	...	4
Mean temp. of warmest quarter	...	...	...	...	...	...
Mean temp. of coldest quarter	...	...	...	...	3	...
Annual precip.	...	...	...	...	...	...
Precip. of wettest month	...	...	...	...	...	...
Precip. of driest month	...	...	...	...	2	...
Precip. seasonality	4	...	...	...	...	3
Precip. of wettest quarter	...	...	...	...	5	...
Precip. of driest quarter	...	...	...	...	...	...
Precip. of warmest quarter	5	2	4	...	1	1
Precip. of coldest quarter	3	...	2	4	...	5
Flow accumulation	...	...	...	...	...	...
Horizontal tide	...	...	...	...	...	...

Note: Other abbreviations are as follows: temperature (temp.), precipitation (precip.), maximum (max.), and minimum (min.). Mean diurnal range is the mean of monthly(maximum temperature − minimum temperature). Isothermality is (mean diurnal range/temperature annual range) multiplied by100. Temperature seasonality is the standard deviation of temperature values multiplied by 100. Temperature annual range is the maximum temperature of the warmest month minus the minimum temperature of the coldest month. Precipitation seasonality is the coefficient of variation of precipitation values. Not all of the 19 bioclimatic predictors listed here were in the top predictor lists for the mangrove species. Ellipses indicate when a variable was not one of the five most important environmental predictors for one of the mangrove species modeled by an individual species distribution model.

Table 3. The five most important environmental predictors identified by general boosted models and the exclusion of correlated variables for *Rhizophora apiculata* (RHAP), *R. mangle* (RHMA), *R. mucronata* (RHMU), *R. racemosa* (RHRA), *R. stylosa* (RHST), and *Sonneratia alba* (SOAL). All of these species' individual distributions were modeled.

Bioclimatic variable	RHAP	RHMA	RHMU	RHRA	RHST	SOAL
Annual mean temp.	...	...	...	...	...	...
Mean diurnal range	...	4	...	4	...	...
Isothermality	...	1	...	...	5	...
Temp. seasonality	5	...	5	2	...	2
Max. temp. of warmest month	...	2	...	...	...	...
Min. temp. of coldest month	...	...	...	...	...	...
Temp. annual range	...	...	...	...	...	...
Mean temp. of wettest quarter	4	...	3	5	1	1
Mean temp. of driest quarter	...	5	...	...	...	...
Mean temp. of warmest quarter	...	...	...	...	...	...
Mean temp. of coldest quarter	...	...	...	...	...	...
Annual precip.	...	...	...	...	...	...
Precip. of wettest month	...	...	...	1	...	...
Precip. of driest month	1	...	...	...	...	...
Precip. seasonality	...	...	...	...	...	4
Precip. of wettest quarter	...	...	...	...	4	...
Precip. of driest quarter	...	...	4	...	...	...
Precip. of warmest quarter	3	...	1	...	3	5
Precip. of coldest quarter	...	3	2	...	...	3
Flow accumulation	2	...	...	...	...	...
Horizontal tide	...	...	...	3	2	...

Table 4. Minimum and maximum longitudinal values of extents used to crop outputs of individual species projections.

Species	Longitude minimum (m)	Longitude maximum (m)
Avicennia germinans	-2.1×10^7	1.8×10^6
Avicennia marina	-1.8×10^6	2.0×10^7
Ceriops tagal	-1.8×10^6	2.0×10^7
Laguncularia racemosa	-2.1×10^7	1.8×10^6
Lumnitzera littorea	7.0×10^6	2.0×10^7
Lumnitzera racemosa	1.8×10^6	2.0×10^7
Rhizophora apiculata	7.0×10^6	2.0×10^7
Rhizophora mangle	-2.1×10^7	1.8×10^6
Rhizophora mucronata	1.8×10^6	2.0×10^7
Rhizophora racemosa	-1.5×10^7	2.0×10^7
Rhizophora stylosa	1.0×10^7	2.0×10^7
Sonneratia alba	1.8×10^6	2.0×10^7

Note: Map projection is Interrupted Goode Homolosine, land-centered.

model's TSS score was calculated using BIO-MOD's default decay value of 1.6 (Thuiller et al. 2009).

Binary (presence/absence) outputs were generated from the continuous outputs of BIOMOD by selecting the threshold that maximized the TSS score. From these data, we calculated the percent of the total number of coastal cells occupied by each species under each scenario. We also calculated the minimum, maximum, mean, and standard deviation of the absolute value of latitude of predicted occurrences for each species. Because the models do not account for dispersal limitation, we cropped model outputs to meaningful regions for each species before summarizing. We used the GBIF data and distribution maps (Spalding et al. 2010) to determine the oceans in which the species occur, and then set projected probabilities to zero at longitudes beyond these regions (Table 4). After selecting crop lines for each species, we examined global projected distributions to ensure that the crop lines did not intersect areas predicted to have continuous occurrences. Thus, summary statistics of model outputs should not be very sensitive to the location of crop lines.

Community distribution models and species richness

Mangroves tend to occur in association with multiple mangrove species, each of which may occur at specific tidal elevations (Macnae 1968). At the coarse scale of this study, we are interested primarily in identifying areas where multi-species mangrove assemblages are likely to occur, rather than distinguishing between different types of mangrove communities. We modeled local species richness ("alpha diversity") because we had inadequate data to model species turnover ("beta diversity").

We modeled mangrove species richness using three different approaches: a composite model, a continuous-response model, and a binary-response model. For the composite model, we combined the independent projections of the 12 individual SDMs by summing the predicted occurrences within each coastal cell. For the continuous and binary models, we calculated the current species richness within each coastal cell based upon all 30 major mangrove species in our GBIF data set (Table 1).

In the binary model, we sought to identify those cells where multi-species mangrove communities are most likely to exist. To do this, we assigned each cell with three or more species out of the 30 total species in our GBIF data a value of one and each cell with less than three species was assigned a value of zero. In this analysis, we modeled presence of cells with high species richness relative to the other cells in our data set. This process yielded 355 presences of high richness cells. We used three species as the threshold because this was the highest value that would yield enough presences of these high richness cells for sufficient predictor-to-response ratios in the models. The presence of three species may not indicate a true hotspot of mangrove diversity in the field. However, this threshold is appropriate within the context of the GBIF data set, and allows us to confidently weed out cells where only one or two mangrove species exist. We considered using different thresholds for defining high richness in the eastern and western hemispheres, because one might expect greater overall richness in the eastern hemisphere. However, we only see more high-richness cells in the east when the threshold is set at four or five species per cell (Fig. 1), at which levels there are insufficient sample sizes. We further felt that it was more appropriate to treat all of the data uniformly in the model, rather than imposing further rules that may introduce more potential for bias.
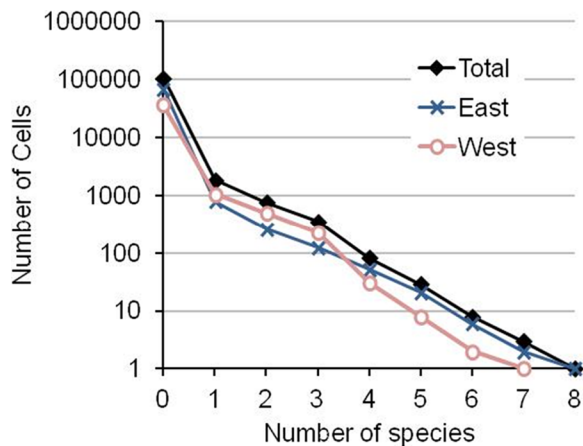
We ran the binary richness data through the

Fig. 1. Number of 4.318 km coastal grid cells containing at least zero to eight mangrove species in the Global Biodiversity Information Facility database. One grid cell in the eastern region had 11 species in it. All other grid cells had fewer than eight species.

same BIOMOD modeling process that we did for each of the individual species. For weights in the binary model, we used the actual number of species observed in each cell (Fig. 1).

For the continuous CDMs, we did not have access to a comprehensive software package for ensemble distribution model selection and prediction based on non-binary data (e.g., BIOMOD does not model abundance). Instead, we fit the full GBM and GLM models using all 21 environmental variables as predictors and the number of mangrove species reported within each grid cell as the response. We compared models with the full suite of predictor variables to those fit using subsets of variables: the five variables with the greatest influence; or by iteratively discarding the least influential variable between pairs of variables with greater than 0.7 correlations and rerunning the model until there were no more correlated environmental variables (Dormann et al. 2012). We used AIC stepwise selection to discard variables that were not significant at the 0.05 level. As we did with the SDMs, the mangrove presence data were combined with pseudo-absences generated by selecting 0, 500, 1000, or 10000 random cells from within 40 kilometers of the entire coastline.

To determine which type of model yielded the best predictive performance, we divided the world into eastern and western regions defined by a longitudinal division through central Africa at 22.46° where there are no recorded mangrove occurrences. We then trained each model on the separate halves of the world and evaluated their predictive performance on the observed data in the other half of the world. To assess predictive performance, we used the likelihood of univariate GLMs comparing observed species richness in the holdout data sets to predicted species richness. Because our ultimate aim was to examine large-scale patterns in mangrove species diversity, we also tested predictive performance of the full GBM and full GLM models at a coarser resolution. In the coarse-resolution tests, we aggregated the predicted and observed data in the holdout regions to a 500-km grid cell size before comparing predicted and observed species densities. For the final selected model, we fit the subset of predictor variables to the entire world, and then projected forward using the environmental variables in the 2080 3 m sea level rise scenario because the results of the SDMs we ran previously were not sensitive to the different sea-level rise scenarios.

For the composite, binary, and continuous CDMs, we generated 500-km grid cell maps of forecasted change in species richness between current conditions and future scenarios. We also calculated means of latitude in each cell weighted by the fitted species richness in current and future scenarios for the three models. The GBM model with the full suite of variables had the best predictive performance in most scenarios (Table 5), and so we used this model for our future projections. As with the SDMs, model evaluation with holdout data suggested that models trained with the least pseudo-absences had the best predictive performance when tested against the data with the original ~4 km (i.e., 2.5 minute) grid size. However, coarse scale maps produced by these models exhibited many nonsensical predictions for current mangrove occurrences, including high species richness in high latitude regions. When examining predictions that had first been re-scaled to a 500 km grid size, inclusion of pseudo-absences improved model likelihoods, and produced maps of current fitted distributions that better matched our expectations. Because our study is focused on global changes in mangrove distributions, we opted for including 2000 pseudo-absences in the final

Table 5. Negative log-likelihoods of continuous community distribution models used to predict mangrove species densities.

Model	Resolution (km)	Training data	Validation data	No. absences	Mean	SD
GBM full	4	East	West	0	−7156	37.0
GBM full	4	West	East	0	−6629	16.0
GBM full	4	East	West	500	−7301	29.0
GBM full	4	West	East	500	−6631	14.0
GBM full	4	East	West	1000	−7380	32.0
GBM full	4	West	East	1000	−6632	13.0
GBM full	4	East	West	2000	−7526	12.0
GBM full	4	West	East	2000	−6655	9.8
GBM full	4	East	West	10000	−7603	2.5
GBM full	4	West	East	10000	−6674	0.6
GBM top 5 variables	4	East	West	0	−7245	49.0
GBM top 5 variables	4	West	East	0	−6670	10.0
GBM top 5 variables	4	East	West	500	−7396	33.0
GBM top 5 variables	4	West	East	500	−6669	4.1
GBM top 5 variables	4	East	West	1000	−7487	32.0
GBM top 5 variables	4	West	East	1000	−6668	8.2
GBM top 5 variables	4	East	West	2000	−7586	13.0
GBM top 5 variables	4	West	East	2000	−6680	7.2
GBM top 5 variables	4	East	West	10000	−7614	2.4
GBM top 5 variables	4	West	East	10000	−6708	0.8
GBM uncorrelated variables	4	East	West	0	−7245	49.0
GBM uncorrelated variables	4	West	East	0	−6670	10.0
GBM uncorrelated variables	4	East	West	500	−7396	33.0
GBM uncorrelated variables	4	West	East	500	−6669	4.1
GBM uncorrelated variables	4	East	West	1000	−7487	32.0
GBM uncorrelated variables	4	West	East	1000	−6668	8.2
GBM uncorrelated variables	4	East	West	2000	−7586	13.0
GBM uncorrelated variables	4	West	East	2000	−6680	7.2
GBM uncorrelated variables	4	East	West	10000	−7614	2.4
GBM uncorrelated variables	4	West	East	10000	−6708	0.8
GLM full	4	East	West	0	−7582	280.0
GLM full	4	West	East	0	−6673	19.0
GLM full	4	East	West	500	−7629	190.0
GLM full	4	West	East	500	−6687	17.0
GLM full	4	East	West	1000	−7554	180.0
GLM full	4	West	East	1000	−6693	9.0
GLM full	4	East	West	2000	−7803	57.0
GLM full	4	West	East	2000	−6711	3.2
GLM full	4	East	West	10000	−7831	1.0×10^{-12}
GLM full	4	West	East	10000	−6721	4.5×10^{-13}
GLM AIC stepwise	4	East	West	0	−7363	57.0
GLM AIC stepwise	4	West	East	0	−6688	31.0
GLM AIC stepwise	4	East	West	500	−7524	68.0
GLM AIC stepwise	4	West	East	500	−6697	28.0
GLM AIC stepwise	4	East	West	1000	−7610	49.0
GLM AIC stepwise	4	West	East	1000	−6705	13.0
GLM AIC stepwise	4	East	West	2000	−7782	20.0
GLM AIC stepwise	4	West	East	2000	−6728	16.0
GLM AIC stepwise	4	East	West	10000	−7844	1.4×10^{-12}
GLM AIC stepwise	4	West	East	10000	−6721	5.6×10^{-13}
GLM significant variables	4	East	West	0	−7276	190.0
GLM significant variables	4	West	East	0	−6664	44.0
GLM significant variables	4	East	West	500	−7414	88.0
GLM significant variables	4	West	East	500	−6694	39.0
GLM significant variables	4	East	West	1000	−7618	75.0
GLM significant variables	4	West	East	1000	−6703	19.0
GLM significant variables	4	East	West	2000	−7803	12.0
GLM significant variables	4	West	East	2000	−6738	6.2
GLM significant variables	4	East	West	10000	−7850	1.3×10^{-12}
GLM significant variables	4	West	East	10000	−6752	3.2×10^{-13}
GLM uncorrelated variables	4	East	West	0	−7724	190.0
GLM uncorrelated variables	4	West	East	0	−6725	29.0
GLM uncorrelated variables	4	East	West	500	−7338	56.0
GLM uncorrelated variables	4	West	East	500	−6725	31.0
GLM uncorrelated variables	4	East	West	1000	−7366	16.0
GLM uncorrelated variables	4	West	East	1000	−6667	48.0
GLM uncorrelated variables	4	East	West	2000	−7492	110.0

GLM uncorrelated variables	4	West	East	2000	−6700	11.0
GLM uncorrelated variables	4	East	West	10000	−7819	3.2×10^{-13}
GLM uncorrelated variables	4	West	East	10000	−6716	0.0
GBM full	500	East	West	0	−2641	2.4
GBM full	500	West	East	0	−2297	0.3
GBM full	500	East	West	500	−2429	22.0
GBM full	500	West	East	500	−2248	4.8
GBM full	500	East	West	1000	−2467	34.0
GBM full	500	West	East	1000	−2244	5.4
GBM full	500	East	West	2000	−2517	31.0
GBM full	500	West	East	2000	−2237	4.6
GBM full	500	East	West	10000	−2640	21.0
GBM full	500	West	East	10000	−2217	4.5
GLM full	500	East	West	0	−2401	0.0
GLM full	500	West	East	0	−2285	0.0
GLM full	500	East	West	500	−2997	650.0
GLM full	500	West	East	500	−2270	7.3
GLM full	500	East	West	1000	−2722	450.0
GLM full	500	West	East	1000	−2275	5.7
GLM full	500	East	West	2000	−2977	410.0
GLM full	500	West	East	2000	−2281	6.2
GLM full	500	East	West	10000	−3192	190.0
GLM full	500	West	East	10000	−2310	5.9

Note: Models were fit using only data from the eastern or western world regions, and then tested against data in the other regions. Values represent negative log-likelihoods of generalized linear models comparing observed species densities to predicted densities in the holdout regions.

model. This yielded an approximate presence to absence ratio of 1:1, similar to that used in the individual SDMs with 500 pseudo-absences. Code for all SDMs and CDMS performed using R statistical software version 14.0 is included in the Supplement.

Evaluation of SDM and CDM outputs

We evaluated model outputs by generating summary maps at a coarser resolution in order to generalize patterns across regions. We generated these maps with 500 km grid cells and 1000 km grid cells. Within each of the larger cells, we summed the predicted species richness in all of the 4 km grid cells. The result is a mangrove species density value for each of the measured cells. This density is different from the mean species richness, because it incorporates both species richness and the number of occupied cells. A 500-km cell centered on Panama has much more coastline than a 500-km cell centered on the coast of Peru. Thus, even if every 4 km coastal cell had the same number of species, the species density measured in the 500 km grid cells would be higher in Panama than Peru.

Coastline versus Latitude

Our study analyzes latitudinal shifts in coastal species. To frame our results, we also needed to understand how the world's coastlines are distributed with respect to latitude. To this end, we summed the total number of ~4 km grid cells within each 2-degree latitudinal bin. We also performed a separate analysis using ArcMap in which we compared the total length of our coastline vector data within 15° of the equator, and between 15° and 30° from the equator. The vector data was generated at a 1.7 km resolution.

RESULTS

Species distribution models

The current distribution of each of the most common 12 mangrove species was best predicted by a different set of five environmental variables (Tables 2 and 3); precipitation in the warmest and coldest quarters appeared in the list of top five predictors for more than half of the mangrove species. In the variable selection process, river discharge and horizontal tide were identified as important environmental predictors only for *Rhizophora apiculata*, *R. racemosa*, and *R. stylosa* (Tables 2 and 3). The predictive performance of
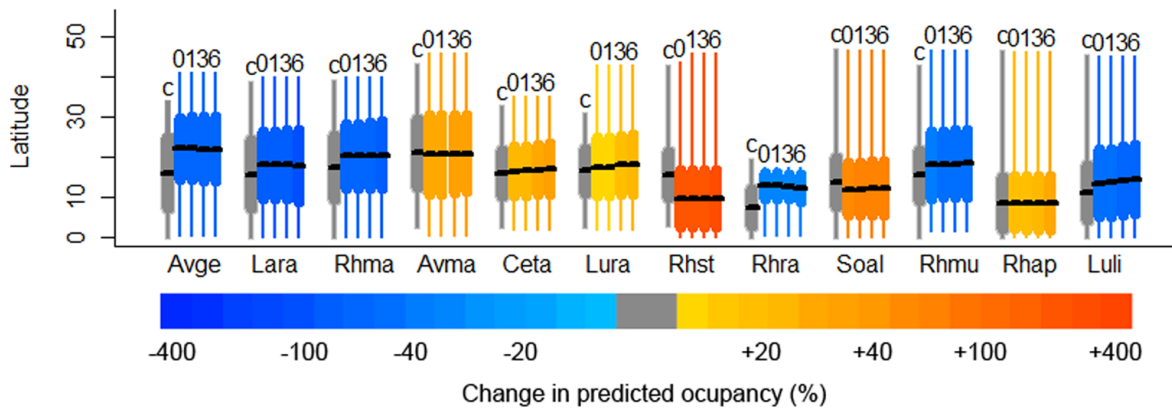
Fig. 2. Predicted latitudinal distributions of 12 mangrove species under each sea-level rise scenario. Thin vertical bars represent minimum and maximum latitudes, thick vertical bars represent standard deviations, and horizontal bars represent means. Labels above each maximum represent the current ('c') fitted distributions as well as the projections for sea level rise of 0 m, 1 m, 3 m, or 6 m. The colors of the projected vertical bars represent the percent change in the total number of predicted occupied cells relative to the current fitted values (see color legend). Species names are as in Table 1. Species are ordered from left to right in decreasing order of the number of GBIF occurrence records.

the models was high: TSS values for the twelve species averaged 0.97 (range 0.950–0.988), but in a few instances the SDMs predicted current mangrove distributions outside of their current known latitudinal range (Fig. 2). Rather than focusing only on minimum and maximum latitudes, we therefore also examined the mean and standard deviations of the absolute values of latitude.

All 12 common mangrove species were forecast to change their absolute mean latitude and total suitable coastal area relative to current climatic conditions (Fig. 2). Half of the modeled species were projected to have a poleward shift of two degrees of latitude or more in the absolute mean latitudes of their distributions under the future climate scenario (Fig. 2). These six species also were forecast to suffer losses in the total area of suitable coastal habitat available within their expanded ranges (Fig. 2). This loss of the amount of suitable coastal habitat available for species with poleward range shifts could be due to the lower amount of total coastline in higher tropical latitudes compared to equatorial areas (Fig. 3). All of the species that did not experience a poleward shift in the absolute mean values of their distributions gained total suitable coastal habitat under the future scenario regardless of the amount of sea-level rise.

The four species with current ranges limited to the Americas, western and central Africa, and the western Pacific islands—*Avicennia germinans*, *Laguncularia racemosa*, *Rhizophora mangle*, *Rhizophora racemosa*—were all forecast to experience overall losses in total suitable coastal habitat and poleward shifts under the future climate scenario compared to current climatic conditions (Figs. 2 and 4–9). The NCAR-CCSM3 GCM forecasts that the annual precipitation in these regions will decrease by at least 50% and that annual temperature will increase by at least 2°C. Our
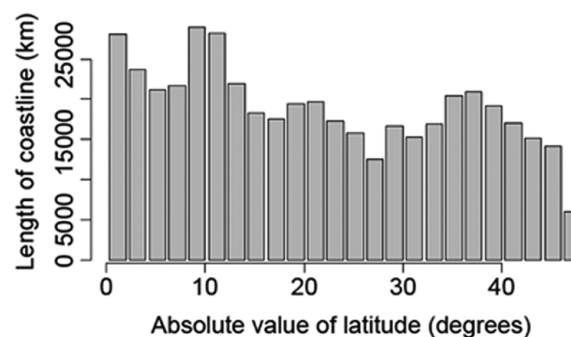

Fig. 3. Length of coastline plotted against absolute value of latitude. Coastline is calculated as the sum of coastal grid cells in our data set multiplied by the cell width (4,318 m).
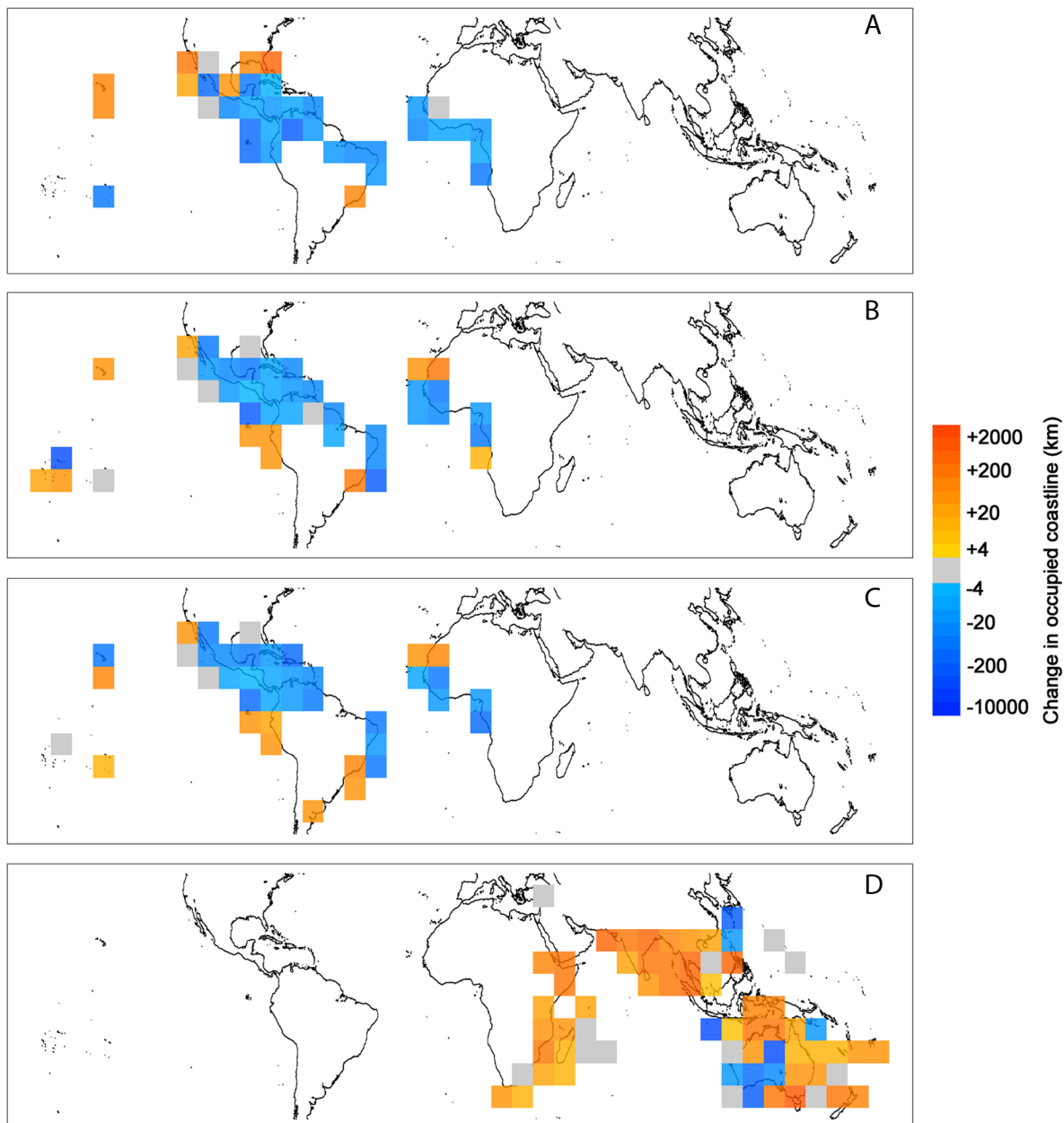
Fig. 4. Change in predicted occupancy for (A) *Avicennia germinans*, (B) *Laguncularia racemosa*, (C) *Rhizophora mangle*, and (D) *Avicennia marina* under the National Center for Atmospheric Research's CCSM3 general circulation model climate scenario projected for 2080 and 3 m of sea-level rise relative to current fitted predicted occupancy. Color shading within each 1,000 km cell represents the change in the number of 2.5-minute cells predicted to contain the focal species. Species in Figs. 4–6 are presented in decreasing order of the number of GBIF occurrence records.

forecasts of mangrove loss in these areas supports previous hypotheses that individual mangrove species' distributions will contract and richness will decline as rainfall and runoff decrease while salinity and extent of acid-sulfide soils increase (Ellison 1994, Snedaker 1995).
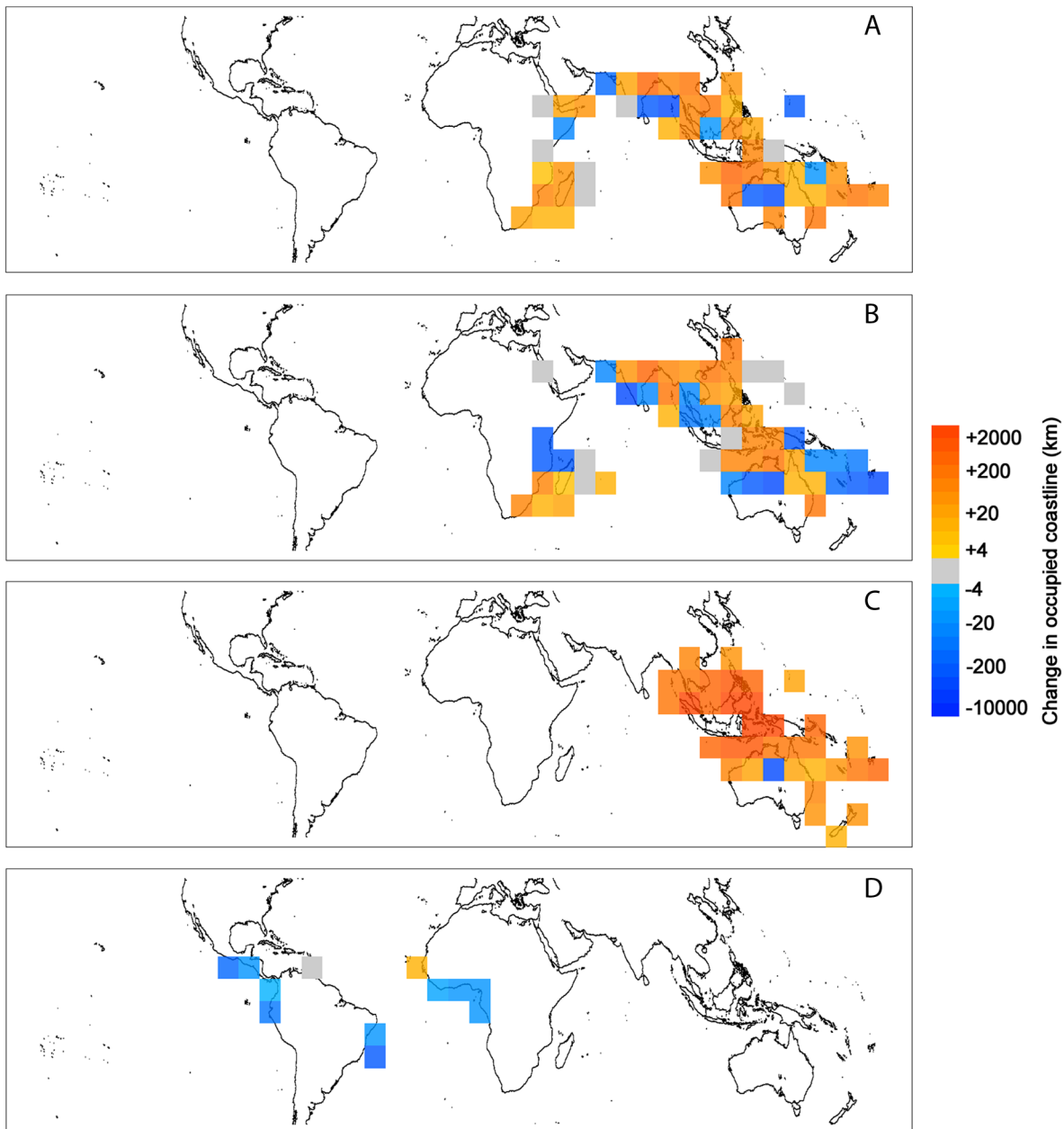
Fig. 5. Change in predicted occupancy for (A) *Ceriops tagal*, (B) *Lumnitzera racemosa*, (C) *Rhizophora stylosa*, and (D) *Rhizophora racemosa* under the National Center for Atmospheric Research's CCSM3 general circulation model climate scenario projected for 2080 and 3 m of sea-level rise relative to current fitted predicted occupancy. Color shading within each 1,000 km cell represents the change in the number of 2.5-minute cells predicted to contain the focal species. Species in Figs. 4–6 are ordered in decreasing order of the number of GBIF occurrence records.

The remaining eight species, with current ranges limited to eastern Africa, Asia, and Australia, had more variable forecasts. *Lumnitzera littorea* and *Rhizophora mucronata* were projected to shift polewards and lose suitable coastal habitat, while *Avicennia marina*, *Ceriops tagal*, *Lumnitzera racemosa*, and *Rhizophora apiculata* were forecasted to gain potential coastal area
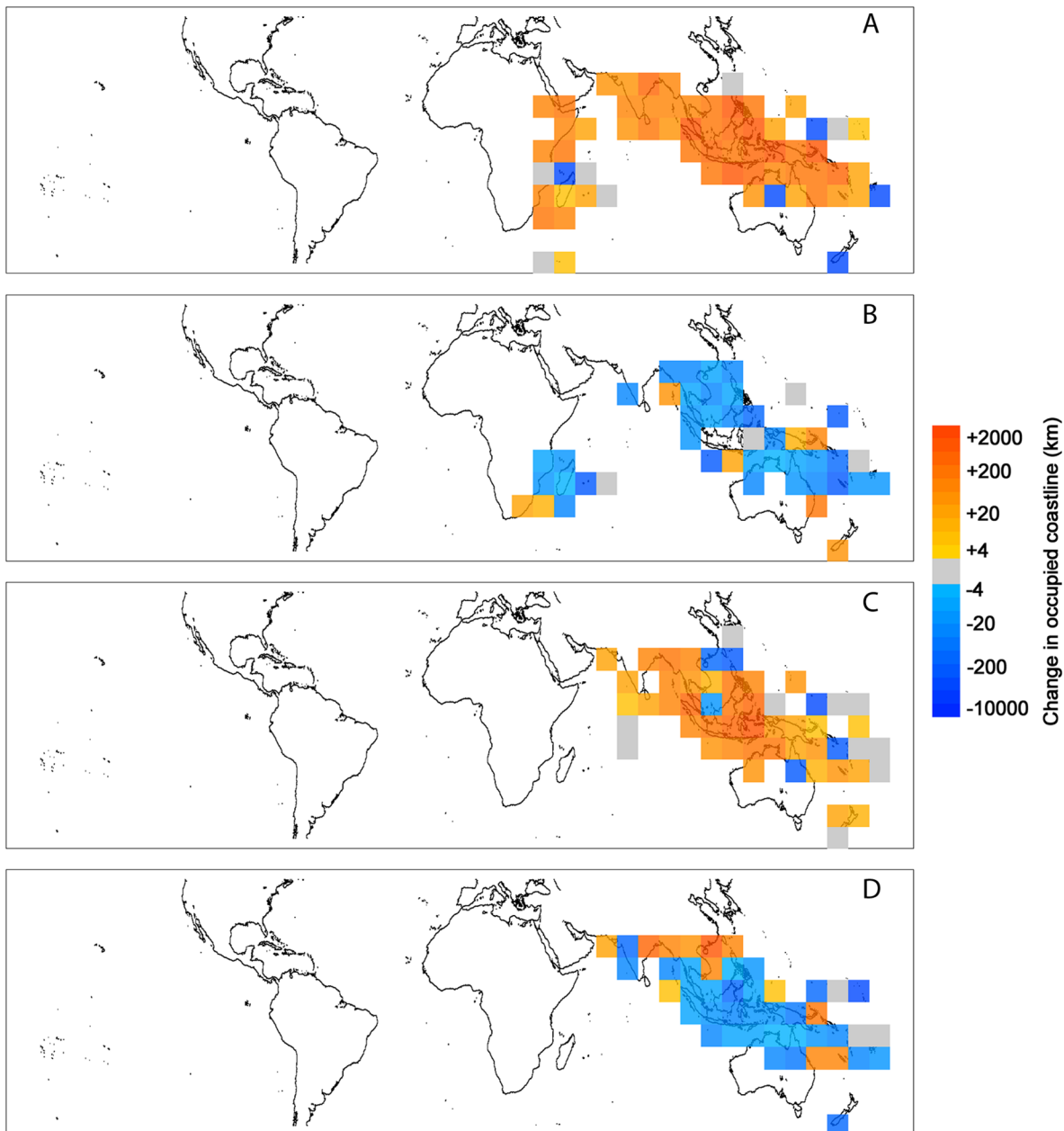
Fig. 6. Change in predicted occupancy for (A) *Sonneratia alba*, (B) *Rhizophora mucronata*, (C) *Rhizophora apiculata*, and (D) *Lumnitzera littorea* under the National Center for Atmospheric Research's CCSM3 general circulation model climate scenario projected for 2080 and 3 m of sea-level rise relative to current fitted predicted occupancy. Color shading within each 1,000 km cell represents the change in the number of 2.5-minute cells predicted to contain the focal species. Species in Figs. 4–6 are ordered in decreasing order of the number of GBIF occurrence records.

with absolute mean latitudinal gains of less than two degrees. *Sonneratia alba* and *Rhizophora stylosa* were projected to gain coastal habitat and experience decreases in absolute mean latitude (i.e., equatorial range contractions). With forecasted gains in suitable coastal area of 260%
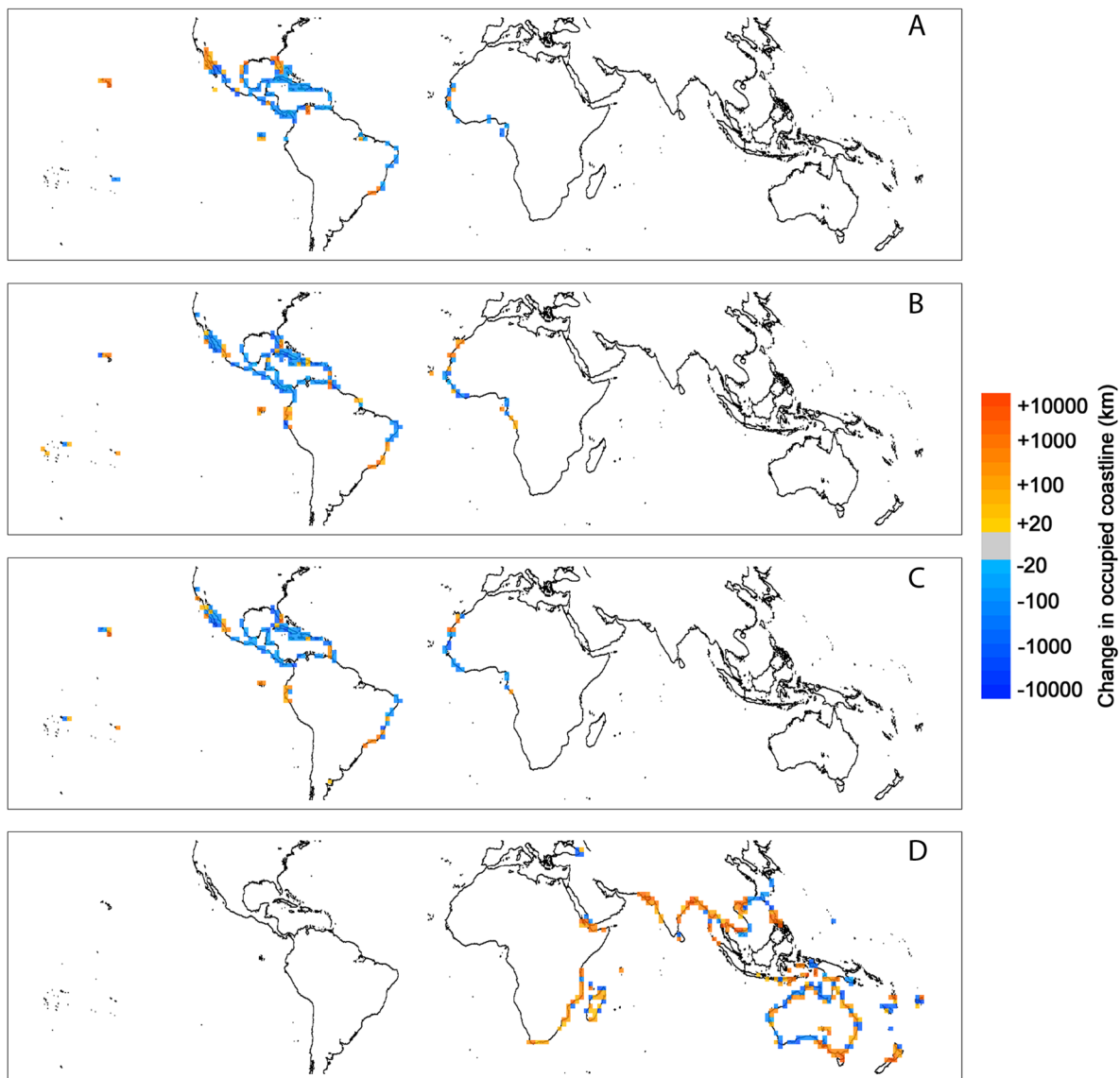
Fig. 7. Change in predicted occupancy for (A) *Avicennia germinans*, (B) *Laguncularia racemosa*, (C) *Rhizophora mangle*, and (D) *Avicennia marina* under the National Center for Atmospheric Research's CCSM3 general circulation model climate scenario projected for 2080 and 3 m of sea-level rise relative to current fitted predicted occupancy. Color shading within each 200 km cell represents the change in the number of 2.5-minute cells predicted to contain the focal species. Species in Figs. 7–9 are ordered in decreasing order of the number of GBIF occurrence records.

to 290% of its current projected distribution, *R. stylosa* was forecast to gain a remarkable 110 to 185% additional habitat relative to its current distribution.

Community distribution models and species richness

The means of the absolute value of latitude weighted by fitted current species density were 14.5°, 14.3° and 17.0° for the composite model, the binary model, and the continuous model, respectively. The projected mean latitudes for the 3m
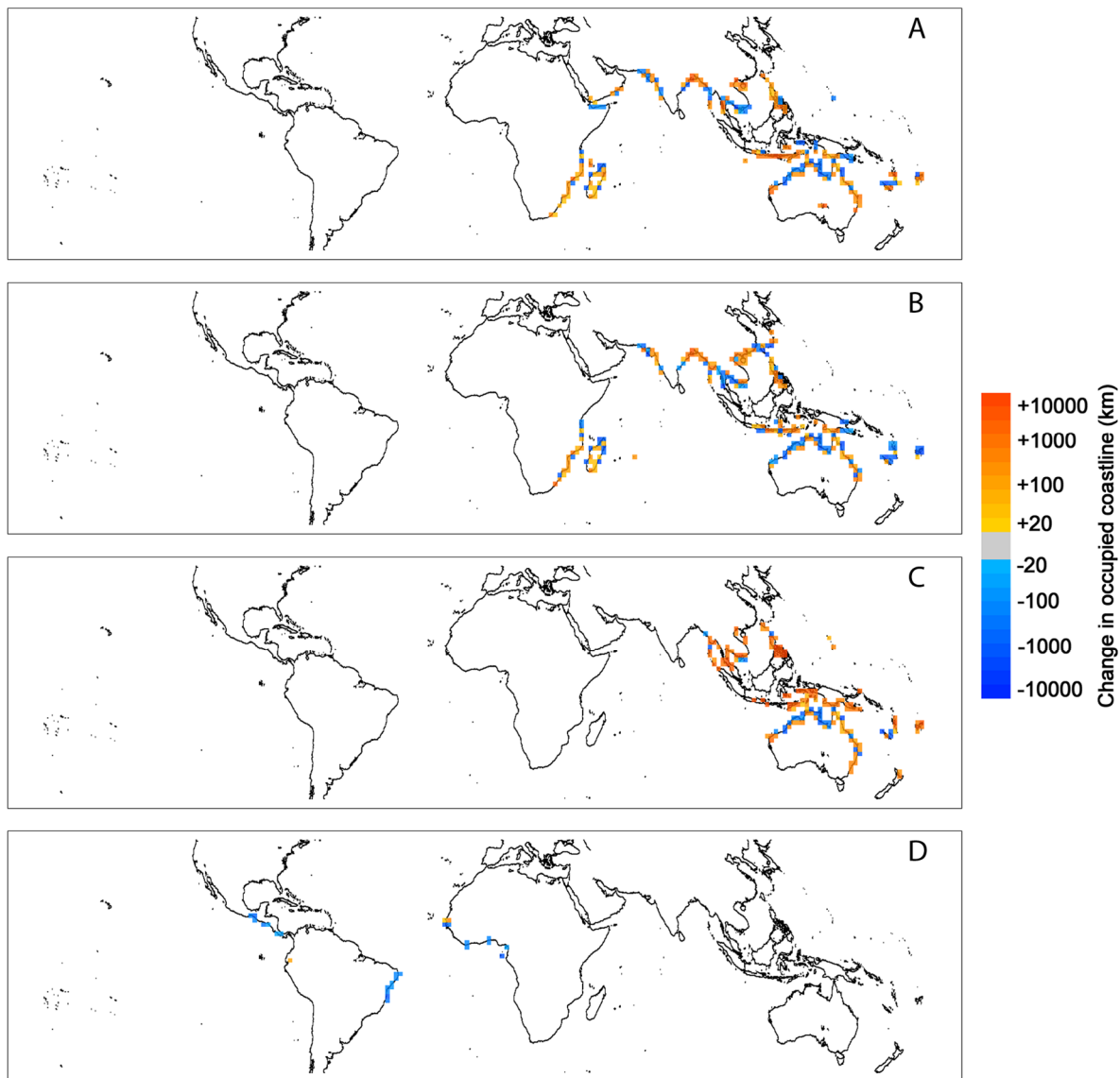
Fig. 8. Change in predicted occupancy for (A) *Ceriops tagal,* (B) *Lumnitzera racemosa,* (C) *Rhizophora stylosa,* and (D) *Rhizophora racemosa* under the National Center for Atmospheric Research's CCSM3 general circulation model climate scenario projected for 2080 and 3 m of sea-level rise relative to current fitted predicted occupancy. Color shading within each 200 km cell represents the change in the number of 2.5-minute cells predicted to contain the focal species. Species in Figs. 7–9 are ordered in decreasing order of the number of GBIF occurrence records.

sea-level rise were 14.6°, 14.2°, and 15.7° for the same three models. The projected maps of change in species density differed between the three model types, although there were a few areas of overlap (Fig. 10). All three models predicted gains in mangrove species density across much of southeastern Asia, southern Brazil, northern Chile, eastern Australia, south-eastern Africa, parts of northern Africa, and parts of northwestern Mexico. All three models also predicted losses of mangrove species density in the Caribbean Islands, parts of Central America and parts of northern Australia (Fig. 10).

Coastline versus latitude
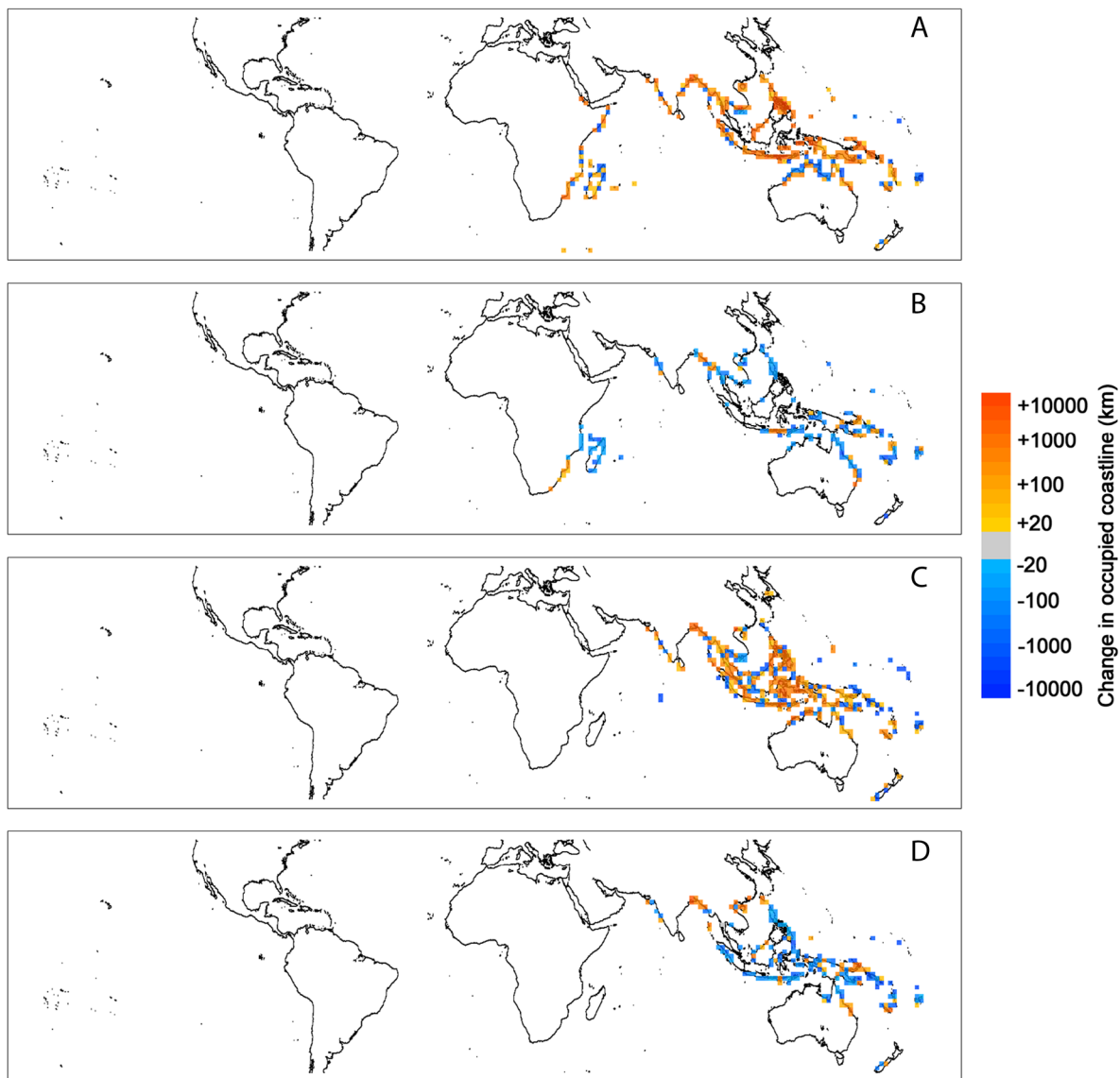
In summing the ~4 km coastal cells vs.

Fig. 9. Change in predicted occupancy for (A) *Sonneratia alba*, (B) *Rhizophora mucronata*, (C) *Rhizophora apiculata*, and (D) *Lumnitzera littorea* under the National Center for Atmospheric Research's CCSM3 general circulation model climate scenario projected for 2080 and 3 m of sea-level rise relative to current fitted predicted occupancy. Color shading within each 200 km cell represents the change in the number of 2.5-minute cells predicted to contain the focal species. Species in Figs. 7–9 are ordered in decreasing order of the number of GBIF occurrence records.

latitude, we found that the total length of coastline between the equator and ±15° was 42% greater than the length of coastline between 15° and 30° N or S (i.e., 182,000 km versus 129,000 km, respectively; Fig. 3). The vector analysis similarly showed 43% more coastline within 15° of the equator than between 15° and 30° from the equator.

DISCUSSION

Species and community distribution models are widely used techniques for evaluating the potential impacts of climatic change on biodiver-
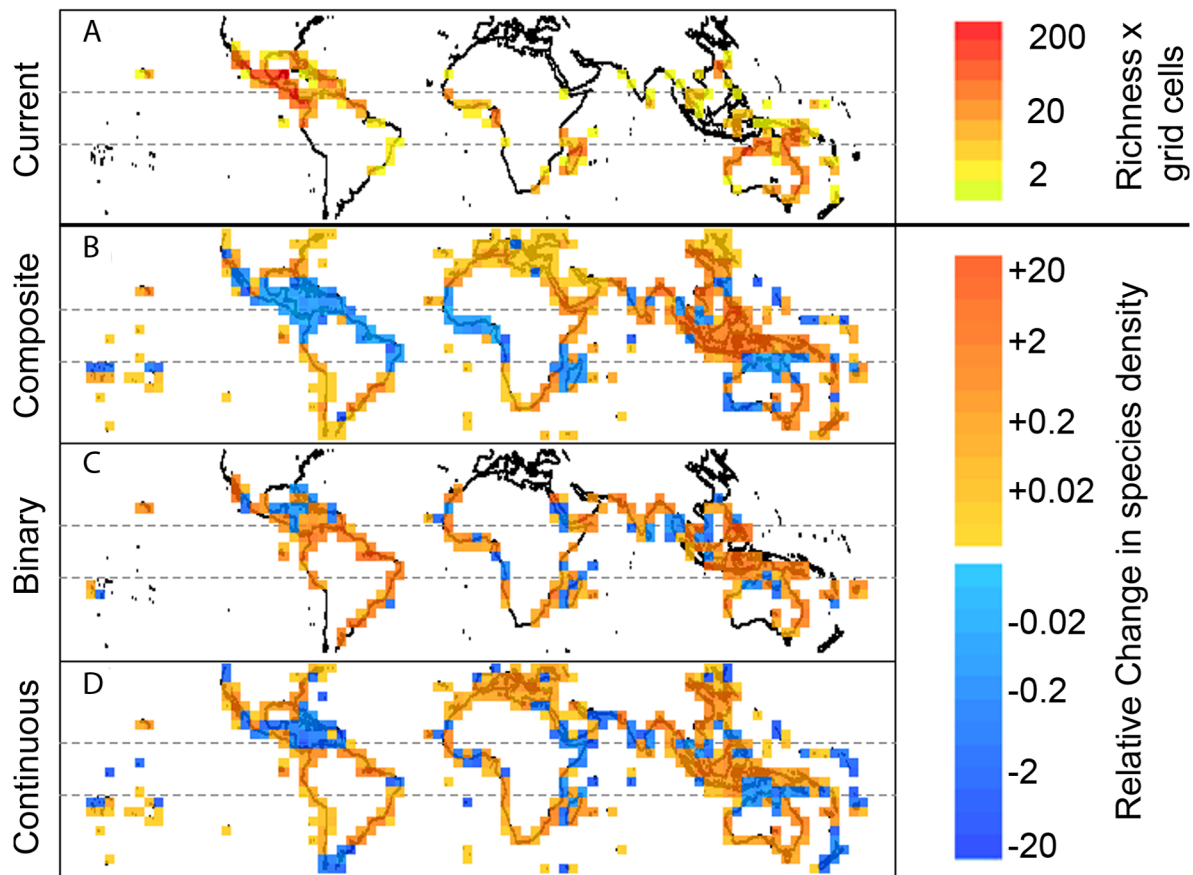
Fig. 10. Change in predicted mangrove species richness in 2080 with a 3 m rise in sea level. Color shading within each 500-km grid cell represents sum over 2.5-minute grid cells of: (A) species richness as observed in the GBIF data; (B) change in the number predicted occupancies for 12 independently modeled species; (C) predicted distribution of mangrove "hot spots" based on a binary model of cells where more than 3 species co-occur; and (D) predicted species richness based on a continuous model of species richness within each cell. The color scale for the three projected maps has been standardized to represent change in future fitted predictions relative to the mean over all cells in the current fitted predictions.

sity (Fitzpatrick et al. 2011). These models use simple correlative relationships to project potential distributions for future climate scenarios in order to inform management and climate-change policy (Hannah et al. 2007). Although distribution models usually perform well in characterizing and predicting current distributions (Franklin and Miller 2009), a number of issues have been raised in regards to the lack of important ecological processes and the methodological issues of such models (e.g., Pearson and Dawson 2003, Record et al. 2013). Previous mangrove species distribution modeling research has been performed at geographic extents much smaller

than the ranges of the species modeled (Cohen et al. 2005, Gilman et al. 2007). The work presented here is the first application of species and community distribution modeling to provide a first approximation of how future climate-change scenarios will influence global distributions of mangrove species and assemblages at geographic extents encompassing the entirety of species' ranges. Understanding the response of mangrove distributions to climate change is timely because mangroves are substantial potential carbon sinks (Siikamäki et al. 2012). Our results provide insights into the effort to understand how coastal organisms, such as mangroves, will be impacted

by climate change at the global level. Our study also highlights some of the methodological limitations and untested ecological assumptions of distribution models.

First, we found that species projected to shift their ranges polewards by at least 2 degrees of latitude consistently experience a decrease in the amount of suitable coastal area available to them. Previous studies have suggested that mangroves will occupy higher latitudes in a warmer climate because current mangrove distributions are limited to the 16°C isotherm for annual temperature of the coldest month (Ellison 1994, Alongi 2008, Gilman et al. 2008), but the link between mangrove distributional shifts and coastal area losses at higher latitudes has not been previously explored.

Second, Central America and the Caribbean are forecast to suffer a greater loss of mangrove species density than other parts of the world. Three of the four species exhibiting declines in Central America and the Caribbean are the best represented species in the GBIF dataset, suggesting that our forecasts for these species are more robust than those for species with sparser occurrence records, such as many species in the Indo-West Pacific (Table 1). Continued contributions of quality georeferenced occurrence records by researchers is imperative to improving our understanding of whether the variation we see in species forecasted distributions in locations such as the Indo-West Pacific are realistic or reflect only artifacts of sampling and reporting.

Third, our study also highlights the importance of considering spatial scale (both grain size and extent) in SDMs. Past studies have demonstrated that mangroves are sensitive to factors including sea-level rise, tidal zones, and river discharge (Ellison and Farnsworth 1997, Ye et al. 2003, reviewed by Duke et al. 1998, Gilman et al. 2007, Alongi 2008). However, these forces are primarily important in influencing the distribution of individual mangrove species at relatively small scales. At larger scales, these relationships break down in the field (Bunt 1996, Ellison et al. 2000), and this breakdown is reflected in the coarser-scale (500-km grid cell) analysis of our community distribution models.

For researchers hoping to advance techniques for distribution models based on continuous data, our model selection process offers a further lesson in considering spatial scale. We found that the extent and grain size at which continuous model outputs are examined, independent of the grain size at which the models operate, can dramatically influence the number of pseudo-absences needed for optimal parameterization. That small scales are best modeled without pseudo-absences, but large-scale models are benefited by pseudo-absence is somewhat intuitive. Without pseudo-absences, the models evaluate finer scale differences within sites occupied by mangroves, whereas with many pseudo-absences, the models can better evaluate the coarser scale differences between areas with and without mangroves. This issue should only apply to continuous data where all presences are not identical, unlike in binary data.

The SDMs and CDMs presented here provide a first approximation of how mangroves will respond to climate change given simple correlative relationships between occurrence records and environmental data (Peterson et al. 2011). In reality, additional factors, such as coastal development, forestry, and biotic processes (e.g., propagule dispersal, recruitment limitation, interspecific competition, and plant-animal interactions) will also play important roles in structuring future mangrove distributions (e.g., Rabinowitz 1978, Clarke and Kerrigan 2002, Farnsworth and Ellison 1997b, Ellison 2008). Our modeling forecasts are thus optimistic because they assume that species will occur wherever the environmental conditions are suitable for them and these other processes will remain constant (cf. Farnsworth and Ellison 1997a). Future studies in which researchers across the world collaborate to provide consistent data on such biotic and social drivers of mangrove distributions across a range of spatial and temporal scales (Farnsworth 1998) would help to make it possible to better understand and model the future fate of mangroves in a global context.

Acknowledgments

Literature Cited

Allouche, O., A. Tsoar, and R. Kadmon. 2006. Assessing the accuracy of species distribution models: prevalence, kappa, and the true skill statistic. Journal of Applied Ecology 43:1223–1232.

Alongi, D. M. 2008. Mangrove forests: resilience, protection from tsunamis, and responses to global climate change. Estuarine, Coastal and Shelf Science 76:1–13.

Araujo, M. B. and M. New. 2007. Ensemble forecasting of species distributions. Trends in Ecology and Evolution 22:42–47.

Barbet-Massin, M., F. Jiguet, C. H. Albert, and W. Thuiller. 2012. Selecting pseudo-absences for species distribution models: how, where, and how many? Methods in Ecology and Evolution 1:1–12.

Berger, U., V. H. Rivera-Monroy, T. W. Doyle, F. Dahdouh-Guebas, N. C. Duke, M. L. Fontalvo-Herazo, H. Hildenbrandt, N. Koedam, U. Mehlig, C. Piou, and R. R. Twilley. 2008. Advances and limitations of individual-based models to analyze and predict dynamics of mangrove forests: a review. Aquatic Botany 89:260–274.

Berger, U., and H. Hildenbrandt. 2000. A new approach to spatially explicit modeling of forest dynamics: spacing, ageing and neighbourhood competition of mangrove trees. Ecological Modelling 132:287–302.

Bromwich, D. H., and J. P. Nicolas. 2010. Sea-level rise: ice sheet uncertainty. Nature Geoscience 3:596–597.

Bunt, J. S. 1996. Mangrove zonation: an examination of data from seventeen riverine estuaries in tropical Australia. Annals of Botany 78:333–341.

Chen, R. and R. R. Twilley. 1998. A gap dynamic model of mangrove forest development along gradients of soil salinity and nutrient resources. Journal of Ecology 86:37–51.

Clarke, P. J., and R. A. Kerrigan. 2002. The effects of seed predators on the recruitment of mangroves. Journal of Ecology 90:728–736.

Clarke, P. J. 1995. The population dynamics of the mangrove *Avicennia marina*: demographic synthesis and predictive modeling. Hydrobiologia 295:83–88.

Cohen, M. C. L., P. W. M. Souza Filho, J. L. Ruben, H. Behling, and R. J. Angulo. 2005. A model of Holocene mangrove development and relative sea-level changes on the Braganca Peninsula (northern Brazil). Wetlands Ecology and Management 13:433–443.

Das, S., and J. R. Vincent. 2009. Mangroves protected villages and reduced death toll during Indian super cyclone. Proceedings of the National Academy of Science 106:7357–7360.

Dormann, C. F., et al. 2012. Collinearity: a review of methods to deal with it and a simulation study evaluating their performance. Ecography 35:1–20.

Duke, N. C., M. C. Ball, and J. C. Ellison. 1998. Factors influencing biodiversity and distributional gradients in mangroves. Global Ecology and Biogeography 7:27–47.

Ellison, A. M. 2008. Managing mangroves with benthic diversity in mind: moving beyond roving banditry. Journal of Sea Research 59:2–15.

Ellison, A. M. 2002. Macroecology of mangroves: large-scale patterns and processes in tropical forests. Trees—Structure and Function 16:181–194.

Ellison, A. M., B. B. Mukherjee, and A. Karim. 2000. Testing patterns of zonation in mangroves: scale dependence and environmental correlates in the Sundarbans of Bangladesh. Journal of Ecology 88:813–824.

Ellison, A. M., and E. J. Farnsworth. 1997. Simulated sea level change alters anatomy, physiology, growth, and reproduction of red mangrove (*Rhizophora mangle* L.). Oecologia 112:435–446.

Ellison, J. C. 1994. Climate change and sea-level rise impacts on mangrove ecosystems. Pages 11–30 *in* J. Pernetta, R. Leemans, D. Elder, and S. Humphrey, editors. Impacts of climate change on ecosystems and species: marine and coastal systems. IUCN, Gland, Switzerland.

Ellison, J. C. 1993. Mangrove retreat with rising sea-level, Bermuda. Estuarine, Coastal, and Shelf Science 37:75–87.

Elith, J., J. R. Leathwick, and T. Hastie. 2008. A working guide to boosted regression trees. Journal of Animal Ecology 77:802–813.

Farnsworth, E. J. 1998. Issues of spatial, taxonomic and temporal scale in delineating links between mangrove density and ecosystem function. Global Ecology and Biogeography Letters 7:14–25.

Farnsworth, E. J., and A. M. Ellison. 1997a. Global conservation status of mangrove ecosystems. Ambio 26:328–334.

Farnsworth, E. J., and A. M. Ellison. 1997b. Global patterns of pre-dispersal propagule predation in mangrove forests. Biotropica 29:318–330.

Farnsworth, E. J., A. M. Ellison, and W. K. Gong. 1996. Elevated CO_2 alters anatomy, physiology, growth, and reproduction of red mangrove (*Rhizophora mangle* L.). Oecologia 108:599–609.

Fitzpatrick, M. C., N. J. Sanders, S. Ferrier, J. T. Longino, M. D. Weiser, and R. Dunn. 2011. Forecasting the future of biodiversity: a test of single- and multi-species models for ants in North America. Ecography 34:836–847.

Franklin, J., and J. A. Miller. 2009. Mapping species distributions: spatial inference and prediction. Cambridge University Press, Cambridge, UK.

Friedman, J. H. 2001. Greedy function approximation: a gradient boosting machine. Annals of Statistics 29:1189–1232.

Gilman, E. L., J. Ellison, N. C. Duke, and C. Field. 2008.

Threats to mangroves from climate change and adaptation options. Aquatic Botany 89:237–250.

Gilman, E. L., J. Ellison, and R. Coleman. 2007. Assessment of mangrove response to projected relative sea-level rise and recent historical reconstruction of shoreline position. Environmental Monitoring and Assessment 124:105–130.

Grasso, M. 1998. Ecological-economic model for optimal mangrove trade off between forestry and fishery production: comparing a dynamic optimization and a simulation model. Ecological Modelling 112:131–150.

Guisan, A., and W. Thuiller. 2005. Predicting species distribution models: offering more than simple habitat models. Ecology Letters 8:993–1009.

Hannah, L., G. Midgley, S. Andelman, M. Araujo, G. Hughes, E. Martinez-Meyer, R. Pearson, and P. Williams. 2007. Protected area needs in a changing climate. Frontiers in Ecology and the Environment 5:131–138.

Heald, E. J. 1971. The production of organic detritus in a south Florida estuary. University of Miami Sea Grant Bulletin 6:1–10.

Hijmans, R. J., S. E. Cameron, J. L. Parra, P. G. Jones, and A. Jarvis. 2005. Very high resolution interpolated climate surfaces for global land areas. International Journal of Climatology 25:1965–1978.

IPCC. 2007. Climate change 2007: synthesis report. Contributions of working groups I, II, and III to the Fourth Assessment Report of the Intergovernmental Panel on Climate Change. IPCC, Geneva, Switzerland.

Khatiresan, K., and B. L. Bingham. 2001. Biology of mangroves and mangrove ecosystems. Advances in Marine Biology 40:81–251.

Le Quéré, C., et al. 2009. Trends in the sources and sinks of carbon dioxide. Nature Geoscience 689:1–6.

Lyard, F., F. Lefevre, T. Letellier, and O. Francis. 2006. Modelling the global ocean tides: modern insights from FES2004. Ocean Dynamics 56:394–425.

Lobo, J. M., A. Jiménez-Valverde, and J. Hortal. 2010. The uncertain nature of absences and their importance in species distribution modeling. Ecography 33:103–114.

Macnae, W. 1968. A general account of the fauna and flora of mangrove swamps and forests in the Indo-West-Pacific region. Advances in Marine Biology 6:73–270.

Nicholls, R. J., P. P. Wong, V. R. Burkett, J. O. Codignotto, J. R. Hay, R. F. Mclean, S. Ragoonaden, and C. D. Woodroffe. 2007. Coastal systems and low-lying areas. Climate change 2007: impacts and vulnerability. Contribution of Working Group II to the Fourth Assessment Report of the Intergovernmental Panel on Climate Change. Cambridge University Press, Cambridge, UK.

Odum, W. E., and E. J. Heald. 1975. The detritus-based food web of an estuarine mangrove community. Pages 265–286 in L. E. Cronin editor. Estuarine research. Academic Press, New York, New York, USA.

Pearson, R. G., and T. P. Dawson. 2003. Predicting the impacts of climate change on species distributions: are bioclimate envelope models useful? Global Ecology and Biogeography 12:361–371.

Peterson, A. T., J. Soberón, R. G. Pearson, R. P. Anderson, E. Martínez-Meyer, M. Nakamura, and M. B. Araújo. 2011. Ecological niches and geographic distributions. Princeton University Press, Princeton, New Jersey, USA.

Phillips, S. J., M. Dudik, J. Elith, C. H. Graham, A. Lehmann, J. Leathwick, and S. Ferrier. 2009. Sample selection bias and presence-only distribution models: implications for background and pseudo-absence data. Ecological Applications 19:181–197.

R Development Core Team. 2011. R: a language and environment for statistical computing. R Foundation for Statistical Computing, Vienna, Austria.

Rabinowitz, D. 1978. Dispersal properties of mangrove propagules. Biotropica 10:47–57.

Record, S., M. C. Fitzpatrick, A. O. Finley, S. D. Veloz, and A. M. Ellison. 2013. Should species distribution models account for spatial autocorrelation? A test of model projections across eight millennia of climate change. Global Ecology and Biogeography, in press. doi: 10.111/geb.12017

Rönnbäck, P. 1999. The ecological basis for economic value of seafood production supported by mangrove ecosystems. Ecological Economics 29:235–252.

Siikamäki, J., J. N. Sanchirico, and S. L. Jardine. 2012. Global economic potential for reducing carbon dioxide emissions from mangrove loss. Proceedings of the National Academy of Sciences 109:14369–14374.

Snedaker, S. C. 1995. Mangroves and climate change in the Florida and Caribbean region: scenarios and hypotheses. Hydrobiologia 295:43–49.

Spalding, M., M. Kainuma, and L. Collins. 2010. World atlas of mangroves. Earthscan, London, UK.

Stockwell, D. and D. Peters. 1999. The GARP modeling system: problems and solutions to automated spatial prediction. International Journal of Geographic Information Science 13:143–158.

Thuiller, W., B. Lafourcade, R. Engler, and M. B. Araújo. 2009. BIOMOD—a platform for ensemble forecasting of species distributions. Ecography 32:369–373.

Tomlinson, P. B. 1986. The botany of mangroves. Cambridge University Press, Cambridge, UK.

Twilley, R. R., V. H. Rivera-Monroy, R. Chen, and L. Botero. 1999. Adapting an ecological mangrove

model to simulate trajectories in restoration ecology. Marine Pollution Bulletin 37:404–419.

Walters, B. B., P. Rönnbäck, J. M. Kovacs, B. Crona, S. Ainul Hussain, R. Badola, J. H. Primavera, E. Barbier, and F. Dahdouh-Guebas. 2008. Ethnobiology, socio-economics and management of mangrove forests: a review. Aquatic Botany 89:220–236.

Wisz, M. S. and A. Guisan. 2009. Do pseudo-absence selection strategies influence species distribution models and their predictions? An information-theoretic approach based on simulated data. BMC Ecology 9:8.

Ye, Y., N. F. Y. Tam, Y. S. Wong, and C. Y. Lu. 2003. Growth and physiological responses of two mangrove species (*Bruguiera gymnorhizza* and *Kandelia candel*) to waterlogging. Environmental and Experimental Botany 49:209–221.

Yesson, C., P. W. Brewer, T. Sutton, N. Caithness, J. S. Pahwa, M. Burgess, W. A. Gray, R. J. White, A. C. Jones, F. A. Bisby, and A. Culham. 2007. How global is the Global Biodiversity Information Facility? PLoS ONE 2:e1124.

SUPPLEMENTAL MATERIAL

APPENDIX

The following is a list of the Global Biodiversity Information Facility data contributors. The biodiversity occurrence data were published by: Australian National Herbarium, Berkeley Natural History Museums, Bernice Pauahi Bishop Museum of Natural History, Biologiezentrum Linz Oberoesterreich, Botanic Garden and Botanical Museum Berlin-Dahlem, Botanical Museum Copenhagen, Botanical Research Institute of Texas, Cameroon National Herbarium, Colecciones Instituto Alexander von Humboldt, Comision Nacional para el Conocimiento y Uso de la Biodiversidad de Mexico, Conservation International Rapid Assessment Program Biodiversity Survey Database, Consortium of California Herbaria, Ecole de Faune de Garoua, Fairchild Tropical Botanic Garden, Finnish Museum of Natural History, Flora del Municipio de la Huerta Jalisco, Harvard University Herbaria, Herbario del Jardin Botanic Marimurtra, Herbarium Hamburgense, Herbarium of the Institute of Traditional Medicine Tanzania, Herbarium of the New York Botanical Garden, Herbarium of Plantae TAIF (Tawian e-Learning and Digital Archives Program TELDAP), Herbarium of the University of Aarhus, Herbarium of the University Libre de Bruxelles, Herbarium Universitat Ulm, Herbarium of the University of Zurich, Herbarium Senckenbergianum, Herbario del CIBNOR, Herbario del Instituto de Ecologio Mexico, Herbario los Tuxtlas, Herbario de la Universidad de Granada, Herbario de la Universidad de Salamanca, Herbario SANT Universidad de Santiago de Compostela, Herbier des Conservatoires et Jardins Botaniques de Nancy, Herbier de la Guyane, Herbier du Bacnin, Indian Ocean Node of OBIS, Institut Botanic de Barcelona, Institute of Ecology and Evolutionary Biology National Taiwan University, Instituto de Botanica Daewinion, Instituto de Ciencias Naturales, Instituto de Investigacion Cientifica Tropical, Instituto Nacional de Biodiversidad (INBio) Costa Rica, Kew Royal Botanic Gardens, Taiwan Forestry Research Institute, Louisiana State University Herbarium, Missouri Botanical Garden, Museo Nacional de Costa Rica, Museum National d'Histoire Naturelle, National Herbarium of the Netherlands, National Herbarium of New South Wales, National Museum of Nature and Science Japan, Natural History Museum Vienna, New South Wales Department of Environment Climate Change and Water, New Zealand National Plant Herbarium, Ocean Biogeographic Information System Bioresources Library (OBIS Australia), Phanerogamic Botanical Collections of Sweden, Real Jardin Botanico de Madrid, Royal Botanic Garden Herbarium Edinburgh, Royal Museum of Central Africa, South African National Biodiversity Institute, South Australia Department of Environment and Natural Resources, Southern Cape Herbarium, Taiwan National Museum of Natural Science, Tama Forest Science Garden Forestry and Forest Products Research Institute, Tela-Botanica, TELDAP Endemic Species Research Institute, The European Genetic Resources Catalogue, UNIBIO IBUNAM Collecion de Plantas Acuaticas, United States National Museum of Natural History Botany Collections, Univerisidad de Costa Rica, University of Alabama Biodiversity and Systematics Herbarium, University of Alberta Museums Vascular Plant Herbar-

ium, University of Arizona Herbarium, University of California Davis Herbarium, University of California Santa Barbara Marine Science Institute, University of Connecticut Herbarium, University of Gottingen Herbarium, University of Kansas Biodiversity Research Center, University of Loma Herbarium, University of Montreal Marie-Victorin Herbarium, University of Oregon Museum of Natural and Cultural History, University of Strasbourg Herbarium, University of Tennessee Knoxville, University of Vienna Institute for Botany Herbarium, University of Washington Burke Museum, USDA PLANTS Database, Western Australian Herbarium, Wildlife Institute of India, Yale University Peabody Museum (Accessed through GBIF Data Portal, http://www.data.gbif.org, 2012–03-15).

SUPPLEMENT

R code for single species and community distribution models (*Ecological Archives* C004-004-S1).